ELSEVIER

PII: S0032-3861(97)00343-1

Polymer Vol. 39 No. 4, pp. 855–864, 1998

0032-3861/97/$17.00+0.00

Biodegradable and biocompatible inorganic–organic hybrid materials

2. Dynamic mechanical properties, structure and morphology

D. Tian[a], S. Blacher[b], Ph. Dubois[a,†] and R. Jérôme[a,*]

[a]*Center for Education and Research on Macromolecules (CERM), University of Liège, Sart-Tilman, B6, 4000 Liège, Belgium*

[b]*Service de Génie Chimique, University of Liège, Sart-Tilman, B6, 4000 Liège, Belgium*

(Received 28 October 1996; revised 6 March 1997)

Dynamic mechanical properties, structure and morphology of tetraethoxysilane/poly(ε-caprolactone) (TEOS/PCL) hybrid materials have been analysed by dynamic mechanical spectroscopy, small-angle X-ray scattering, transmission electron microscopy, and image analysis. The experimental observations agree with a microscopic phase separation of the two constitutive components: the organic polymer and the silica network. The effect of the PCL functional end-groups, the number of functional end-groups per PCL chain, the PCL molecular weight and content, and the curing conditions have been studied on the structure and properties of the hybrid materials. Finally, phase morphology has proved to be co-continuous, at least when the weight composition is close to 50% for each component (SiO_2 and PCL), with a characteristic length between the PCL and silica phases of *ca.* 5 nm, as estimated by image analysis of transmission electron micrographs. © 1997 Elsevier Science Ltd.

(Keywords: inorganic–organic hybrid materials; ceramer; poly(ε-caprolactone); sol–gel process; morphology)

INTRODUCTION

It has been recently reported[1–3] that a new biodegradable and biocompatible inorganic–organic hybrid material could be prepared from tetraethoxysilane and end-reactive poly(ε-caprolactone) (TEOS–PCL) by the sol–gel process. Basically, the sol–gel process can be viewed as a two-step network-forming process. Metal or silicon alkoxides, e.g. $Si(OEt)_4$, are hydrolysed with formation of intermediate species of the metal or silicon hydroxide type. These species then undergo a stepwise polycondensation reaction that results in a metal or silicon oxide three-dimensional network. If an organic compound, e.g. an oligomer or polymer chain, contains at least two groups reactive in the sol–gel process (preferably in a terminal position), this reagent can participate in the polycondensation reaction and be incorporated in new inorganic–organic hybrid materials. The main advantage of this alternative route is to endow the inorganic material with specific properties depending on the selected organic component.

Poly(ε-caprolactone) (PCL) is well-known for a unique set of properties, i.e. biocompatibility, permeability and biodegradability[4–7]. Depending on the polymerisation mechanism, PCL can be end-capped by hydroxyl or vinyl groups[8–11], which are reactive toward alkoxysilane[1,3], i.e. a reagent commonly used in the sol–gel process. Nevertheless, even deprived of reactive end-groups, PCL can be successfully incorporated into the silica network, as result of strong hydrogen bonding of the carbonyl ester group with Si–OH groups of the silica network[3].

The extent of the PCL incorporation in the inorganic network depends on several parameters, such as PCL molecular weight, nature and number of functional groups attached to the PCL chain, curing conditions, etc.[3]. *In-vitro* cell culture and biodegradation tests have confirmed that these new inorganic–organic hybrid materials are novel biomaterials endowed with biodegradable and biocompatible properties[2].

This paper deals with the dynamic mechanical properties of these hybrid materials and the analysis of their structure and morphology by small-angle X-ray scattering (SAXS), transmission electron microscopy and image analysis.

EXPERIMENTAL SECTION

Materials

Syntheses of α,ω-hydroxyl PCL (M_n = 2000 and 4000), α,ω-triethoxysilane PCL (M_n = 2000), three-arm star-shaped PCL end-capped with triethoxysilane (M_n = 12000), and PCL bearing 5 mol.% triethoxysilane pendent groups (M_n = 16000) were detailed elsewhere[3]. PCL-diol (M_n = 1250) and PCL-triol (M_n = 900) (Aldrich) were used as received. Tetraethoxysilane (Janssen), hydrochloric acid (12 N) (Lab Chemistry), tetrahydrofuran (Janssen), ethanol (Riedel–de Haen) were also used as received.

Preparation of tetraethoxysilane–poly(ε-caprolactone) hybrid materials

PCL/TEOS mixtures of various compositions were dissolved in THF (20 wt.%) and hydrolysed with a stoichiometric amount of water with respect to the alkoxide functions. HCl was used as a catalyst in a 0.05/1 HCl/TEOS molar ratio. A representative synthesis was as follows. 1.5 g TEOS was added to the α,ω-triethoxysilane PCL (0.5 g, M_n = 2000) solution in THF (10.0 ml) and thoroughly

* To whom correspondence should be addressed.
† Research Associate by the Belgian National Found For the Scientific Research (FNRS).

mixed until a homogeneous solution was formed. Then deionised water (0.54 ml), ethanol (0.80 ml) and HCl (0.01 ml) were added under rapid stirring at ambient temperature for *ca.* 10 min. The clear solution was then cast into a plastic Petri dish and covered with a Parafilm. Based on a preliminary series of gelation experiments it was shown that, after several days depending on the PCL end-groups (hydroxyl or triethoxysilane), the Parafilm was to be removed[1]. The gelified material was then dried under ambient condition for one week and finally cured at 100°C for 2 days prior to testing. These specific conditions were detailed elsewhere[1,3] and proved to be efficient for preventing cracking phenomena and thermal degradation of PCL from occurring. The usual film thickness was 0.1–1 mm.

Characterisation

Dynamic mechanical analysis (DMA) was performed with a Dynamic Mechanical Analyzer (model 983, Du Pont Instruments) within the temperature range of −120°C to 150°C with a heating rate of 3°C min^{-1} and a frequency of 0.5 Hz. Shear storage (G') and loss (G'') moduli (and thus $\tan \delta = G''/G'$) were calculated from the phase shift (δ) at a 0.5 Hz frequency. The typical size of the samples used was 25 mm × 0.15 mm × 5 mm. Although the samples were clamped over a short gauge length, the clamping arrangements are such that the measurement of true shear moduli cannot be ascertained.

Small-angle X-ray scattering (SAXS) measurements were carried out at the 'Laboratoire pour l'Utilisation du Rayonnement Electromagnetique' (LURE; Orsay France) on DCI (D24 station). The size of the X-ray beam (λ = 1.488 Å) at the sample was smaller than 1 mm^2, so that no desmearing of the data was required. The scattered X-rays were detected with an argon–CO_2 gas-filled, one-dimensional position-sensitive detector (with a resolution of 0.4444 mm). The sample-to-detector distance (1151 mm) allowed SAXS data to be recorded in the 0.02 to 0.8 nm^{-1} s range. These data were plotted as relative intensity *versus* s after correction for parasitic scattering and sample absorption. The background scattering was corrected in the standard manner.

Thin films cast on a copper grid were observed with a Philips CM100 transmission electron microscope (TEM). The natural contrast between the organic polymer and the inorganic phase was strong enough for avoiding any specific staining.

The image treatment and the image statistical analysis were performed on a Sun Spark 10 computer with the Noesis software 'Visilog'. TEM micrographs were digitised using a camera and analysing 512 × 512 pixels with 256 grey levels. The digitised images were binarised in order to distinguish the two phases and used for further statistical analysis.

RESULTS AND DISCUSSION

Dynamic mechanical analysis

Effect of the PCL functional end-groups. As previously reported[1,3], triethoxysilane end-groups are more efficient than hydroxyl end-groups in incorporating PCL chains into the silica network, because of a higher reactivity toward TEOS and water. *Figure 1* shows the effect of the PCL end-groups on the dynamic mechanical properties of a silica–PCL hybrid material, or ceramer, containing 20 wt.%

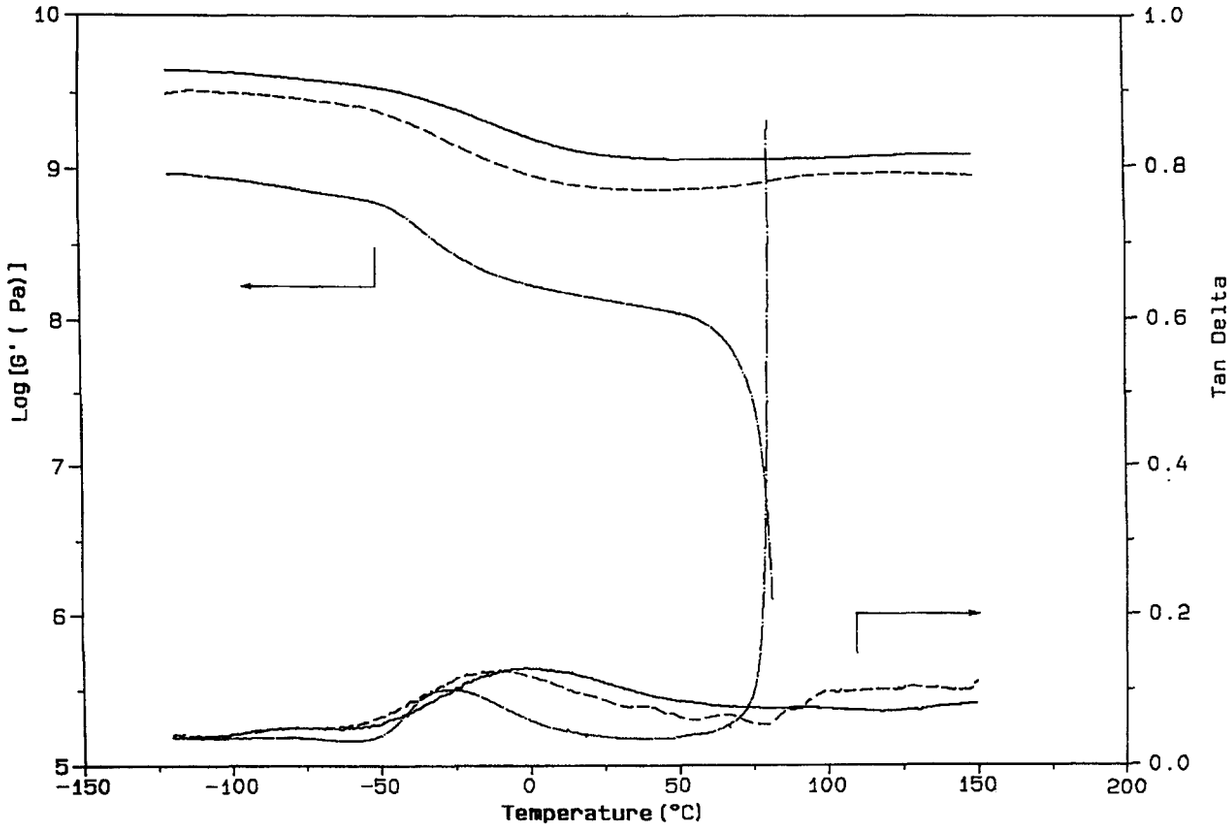

Figure 1 Dynamic mechanical spectra of ceramers prepared from 80 wt.% TEOS and 20 wt.% PCL (M_n = 2000) end-capped at both ends with triethoxysilane groups (———), and hydroxyl groups (- - -). Curves for pure PCL (M_n = 40.0 × 10^3) are also reported (— — —)

PCL and cured for 2 days at 100°C. For the sake of comparison, the temperature dependence of the shear storage modulus (G') and loss factor (tan δ) is shown for pure PCL. The general shape of the G' and tan δ *versus* temperature curves is quite comparable for the ceramers prepared from the end-reactive PCL chains. G' is just slightly higher when the end-groups are triethoxysilane groups rather than hydroxyl ones in the whole temperature range. Nevertheless, G' in the glassy plateau is smaller by half a decade for pure PCL compared to the PCL containing ceramers. The glass transition temperature of PCL is clearly observed, particularly as a maximum in tan δ. The temperature at this maximum is found to increase from pure PCL (−30°C) to −15°C and −4°C for α,ω-hydroxyl PCL and α,ω-triethoxysilane PCL in the ceramers, respectively. Furthermore, this relaxation characteristic of PCL becomes much broader when the polyester is incorporated into the silica network. All these experimental observations agree with a loss of mobility when PCL is part of the ceramer and this effect is as more important as the PCL end-groups are more reactive toward TEOS and water. In contrast to pure PCL, no relaxation is observed in the vicinity of 70°C in case of ceramers, indicating that the polyester is amorphous when intimately incorporated into the silica network. Therefore, beyond T_g of the PCL component, G' of ceramers remains unchanged at least until 150°C. Nevertheless, when α,ω-hydroxyl PCL is reacted with TEOS, a small increase in G' is reported at *ca.* 100°C, which might be consistent with a further reaction of the ceramer. Although broad and of a low intensity, an extra loss peak is observed at *ca.* −80°C for the TEOS/PCL ceramers, whatever the PCL reactive end-groups. Its origin is still unclear and might tentatively be assigned to the beta relaxation of the PCL phase.

Effect of the number of functional end-groups per PCL chain. *Figures 2 and 3* show that the dynamic mechanical behaviour of PCL containing ceramers does not depend importantly on the number of functional end-groups per PCL chain at least at the composition of interest. Two commercially available PCLs, PCL-triol (M_n = 900) and PCL-diol (M_n = 1250), have been used as precursors for the sol–gel process and are compared in *Figure 2*. Both samples show very similar dynamic mechanical curves, i.e. a weak relaxation near −80°C followed by the glass transition of PCL at higher temperature. Although the difference is very small, G' is higher in case of the PCL triol compared to the diol. The same situation prevails in *Figure 3* that compares ceramers containing 20 wt.% PCL bearing zero, two and three reactive end-groups per chain. Indeed, T_g of PCL observed at the maximum of the tan δ peak is the same within the limits of experimental errors, and G' values are quite comparable. It is thus clear that chemical bonding of the PCL chain extremities to the silica network has no determining effect on the properties of the PCL microdomains in the PCL/TEOS ceramers indicating that interactions of the polymer backbone with silica are most important. A previous study by *FT*i.r. has accordingly shown that hydrogen bonding was occurring[3]. In contrast, in a study of poly(tetramethylene oxide) (PTMO)/TEOS ceramers of a 50/50 weight composition, Wilkes *et al.*[12] have observed an effect of the number of functional groups per PTMO chain on the dynamic mechanical properties of the ceramers. For that purpose, pendant hydroxyl

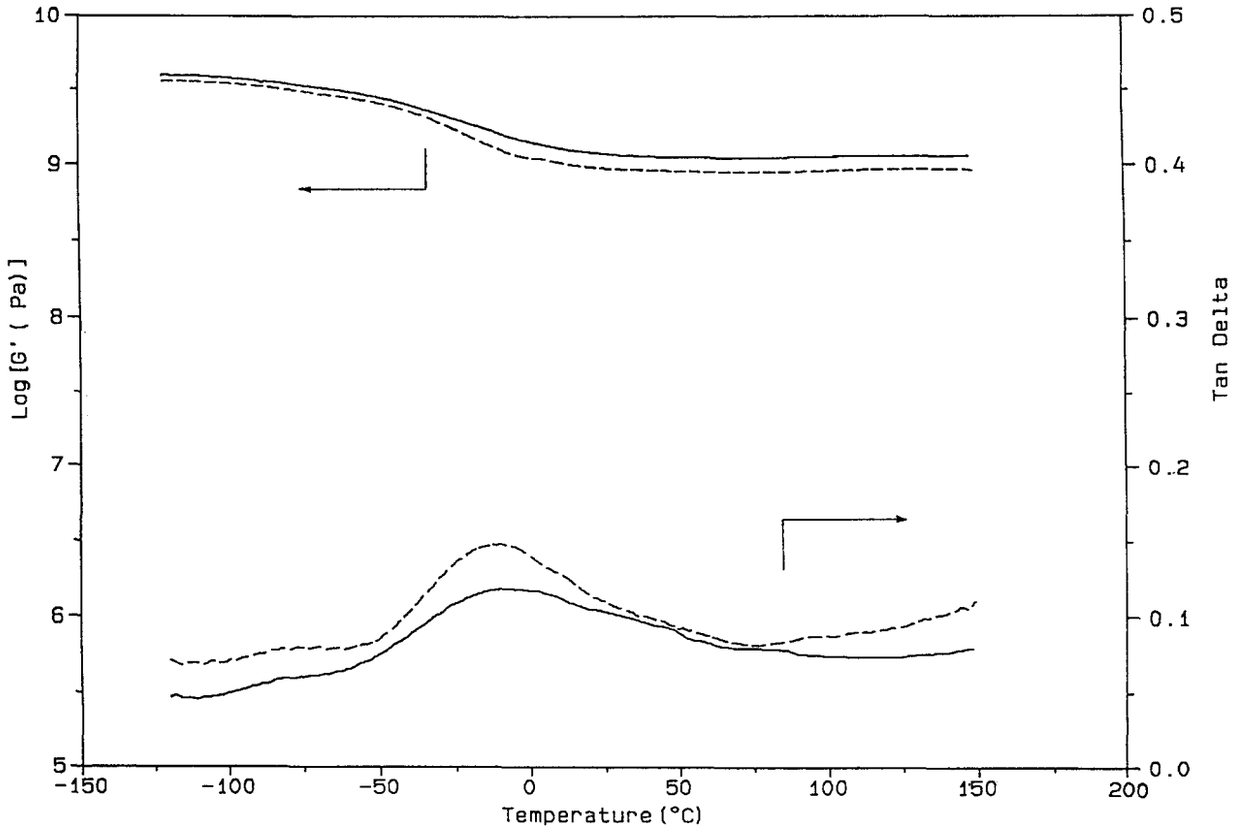

Figure 2 Dynamic mechanical spectra of ceramers prepared from 80 wt.% TEOS and 20 wt.% of PCL-triol (M_n = 900) (———) and PCL-diol (M_n = 1250) (- - -)

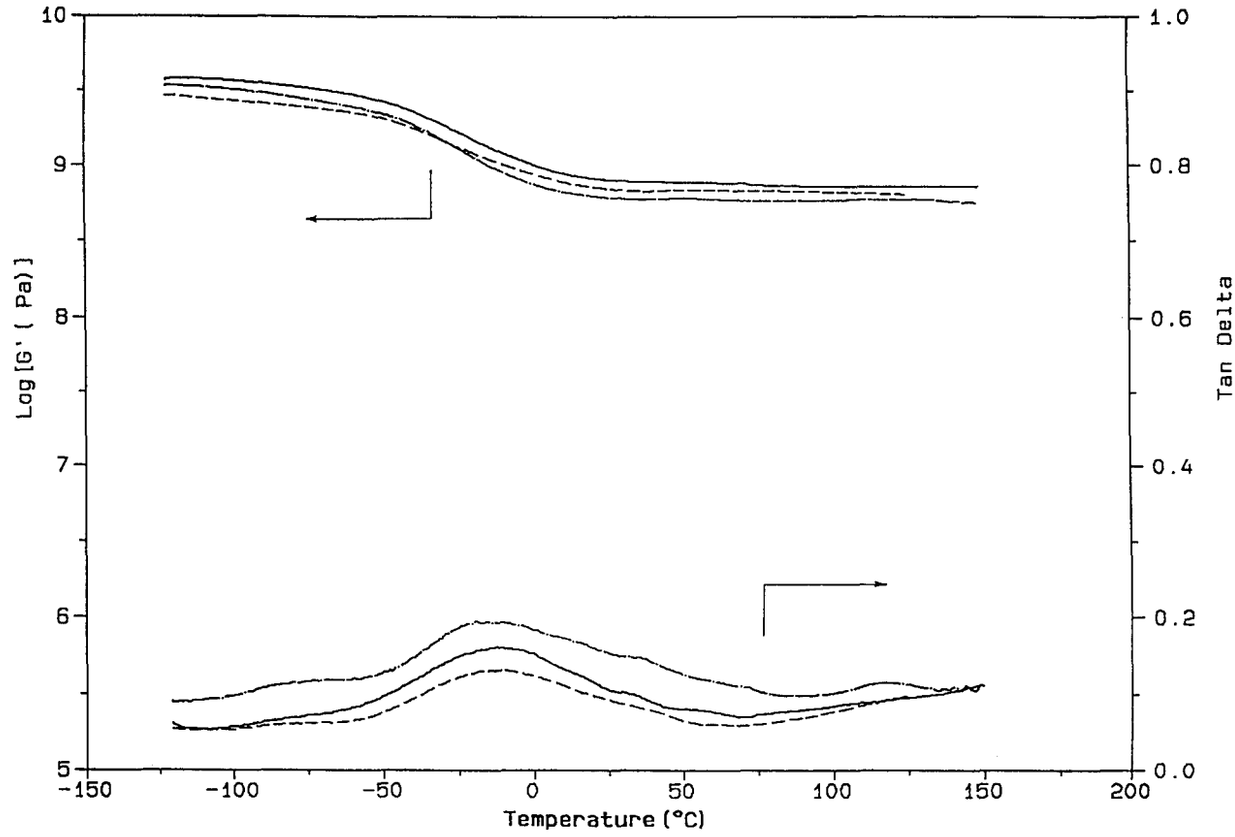

Figure 3 Dynamic mechanical spectra of ceramers prepared from 80 wt.% TEOS and 20 wt.% α,ω-hydroxyl PCL (M_n = 4000) (———), triethoxysilane end-capped three-arm star-shaped PCL (M_n = 12 000) (- - -), and PCL deprived from functional end-groups (M_n = 4000) (— - —)

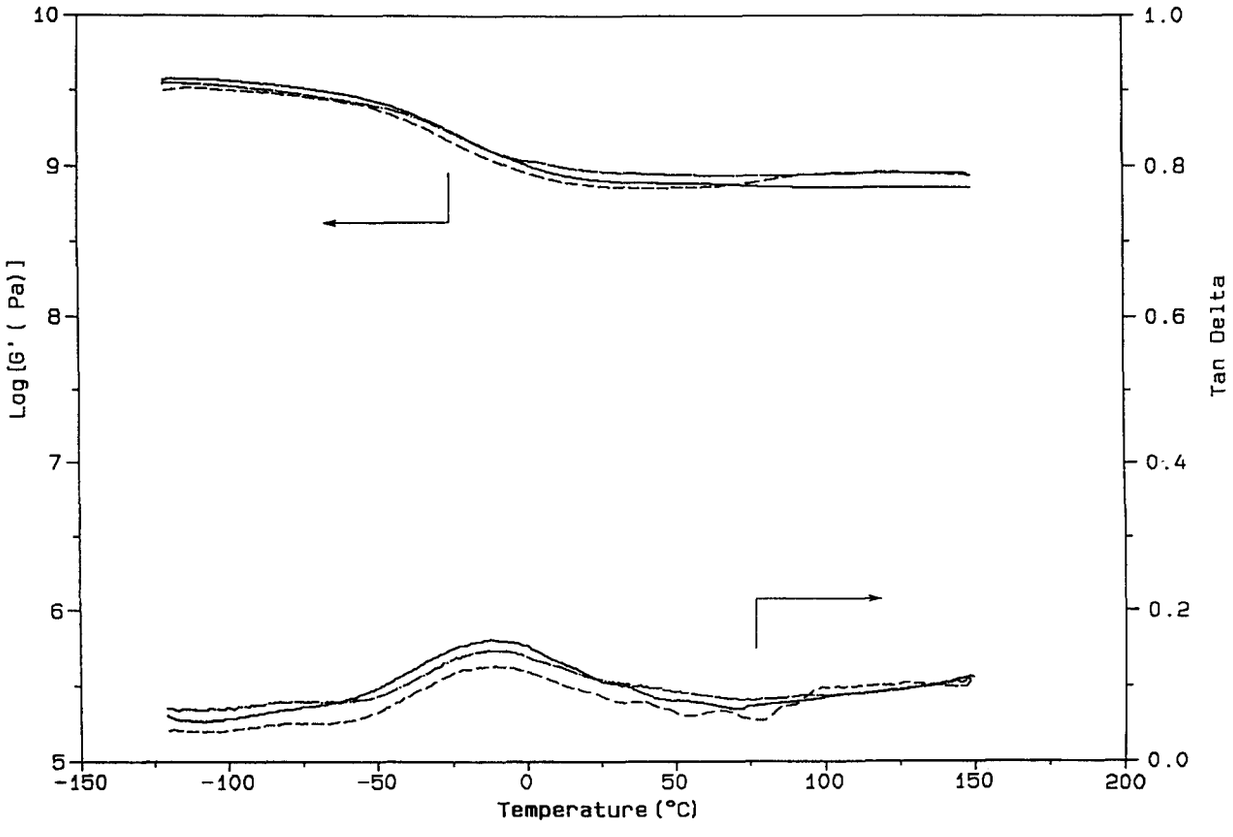

Figure 4 Dynamic mechanical spectra of ceramers prepared from 80 wt.% TEOS and 20 wt.% α,ω-hydroxyl PCL of various molecular weight M_n = 4000 (———), M_n = 2000 (- - -) and M_n = 1250 (— - —)

functionalities have been incorporated by reaction of polytetramethylene oxide diol ($M_n = 1000$), trimethylolpropane and isophorone diisocyanate. This difference with the system studied in this paper might be due to a combination of several parameters: the ceramer composition which contains 80 wt.% TEOS in this study compared to 50 wt.% in the ceramers studied by Wilkes *et al.*, stronger interaction of PCL with silica compared to PTMO and a larger number of reactive groups per PTMO chain (i.e. a maximum of five instead of two for PCL chains).

Effect of the PCL molecular weight. At a constant PCL/TEOS weight composition, any increase in the PCL molecular weight results in a decreasing concentration of the reactive PCL end-groups, but also in a more efficient incorporation of PCL into the silica network[3]. Actually, less TEOS/PCL cross-reactions are required for incorporating the same amount of PCL in the silica network when PCL chains are longer. The dynamic mechanical spectra of ceramers initially containing 20 wt.% α,ω-hydroxyl PCL of increasing molecular weight are again quite comparable (*Figure 4*), which confirms that intermolecular PCL/silica cross-interactions play the decisive role on the PCL chain mobility (T_g) and phase separation.

Effect of the PCL content. Three ceramers of various TEOS contents have been prepared that contain the same α,ω-hydroxyl PCL ($M_n = 4000$). The initial TEOS content was 80, 90 and 95 wt.%, respectively, all the other conditions being kept constant. It has previously been reported[3] that under identical sol–gel conditions, any decrease in the PCL content results in a more efficient PCL incorporation into the silica network and an improved thermal stability of the final ceramers. *Figure 5* shows again a relaxation near −80°C followed by the glass transition of PCL at higher temperature. It is clear that the shear storage modulus increases with the TEOS content. The effect is much more pronounced above T_g of PCL and is quite consistent with the substitute of a stiffer inorganic material for the organic polyester. Also, expectedly, the magnitude of the tan δ peak characteristic of the PCL glass transition rapidly decreases and tends to become broader and shifted toward higher temperature when the PCL content is decreased from 20 to 10 wt.% (*Figure 5*). When 5 wt.% PCL are used, the peak is too weak for reliable conclusions to be drawn. It would thus appear that when the content of the stiff component (silica) is increased, the restrictions imposed on the flexible PCL chains are also more severe consistently with an intimate mixing of the two components. Nevertheless, the transition at ca. − 80°C is still visible when T_g of PCL is no longer observed in the tan δ *versus* temperature curve, which might indicate that this relaxation is characteristic of the inorganic phase.

Effect of the curing conditions. When a sample initially prepared at 25°C is cured at 100°C for 2 days, the tan δ peak for the PCL glass transition is shifted by more than 20°C toward higher temperature, i.e. from −33 up to −11°C. This relaxation is also becoming broader, while the storage modulus above T_g of PCL is significantly increased (*Figure 6*). These experimental observations are in line with the progress of the sol–gel process at a high enough temperature (e.g. 100°C), which is otherwise restricted at 25°C by the early vitrification of the reactive system[1,3]. This further progress in the network formation accounts for the increasing stiffness of the hybrid materials (increase in G') and for more severe restriction on the PCL chain mobility (increase in T_g). No conclusion can be drawn

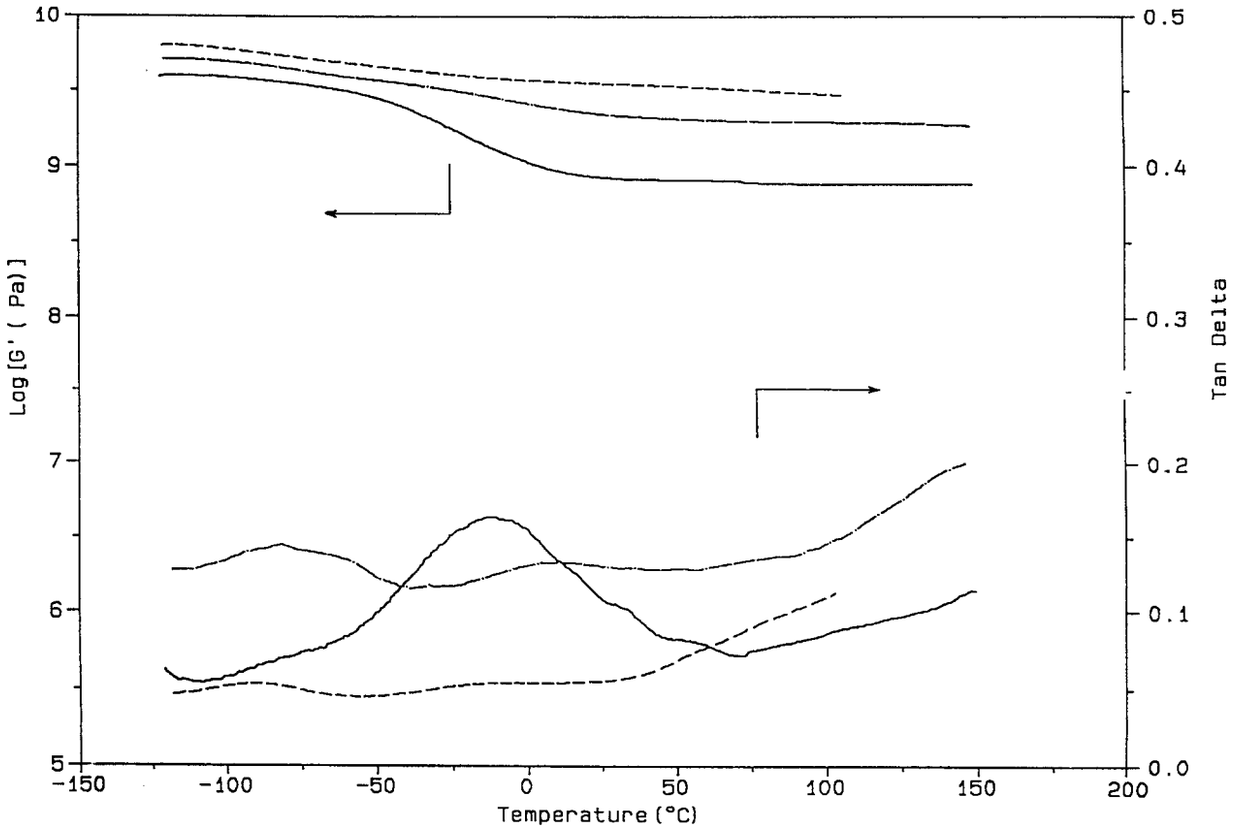

Figure 5 Dynamic mechanical spectra of ceramers prepared from α,ω-hydroxyl PCL ($M_n = 4000$) and various TEOS contents: 80 wt.% (———), 90 wt.% (— - —), and 95 wt.% (- - -)

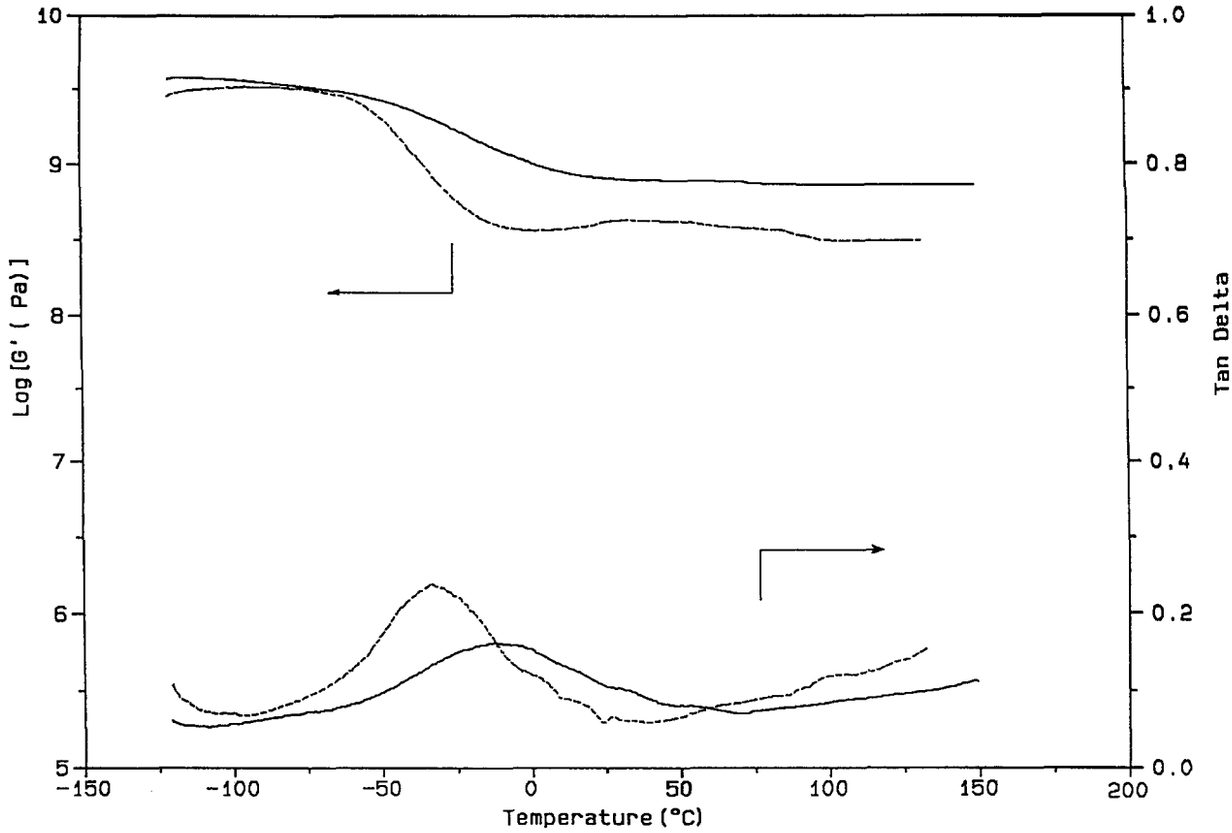

Figure 6 Dynamic mechanical spectra of ceramers prepared from 80 wt.% TEOS and 20 wt.% α,ω-hydroxyl PCL (M_n = 4000) under different curing conditions: 25°C (- - -), and 100°C (———) for 2 days

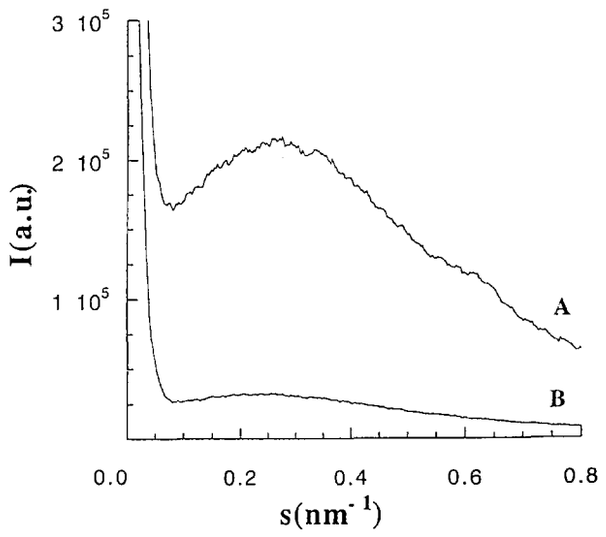

Figure 7 SAXS profiles of ceramers prepared from 80 wt.% TEOS and 20 wt.% α,ω-hydroxyl PCL (M_n = 4000) for different curing conditions: 25°C (a), 100°C (b), for 2 days

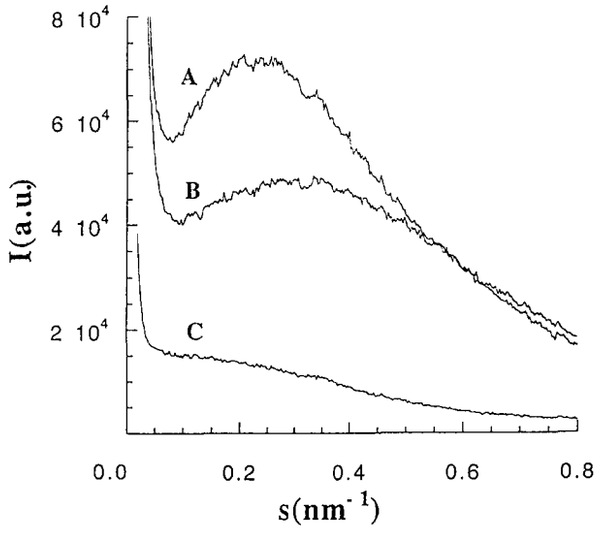

Figure 8 SAXS profiles of ceramers prepared from α,ω-triethoxysilane PCL (M_n = 2000) and various TEOS contents: 80 wt.% (a), 90 wt.% (b), and 95 wt.% (c)

about the effect of curing on the relaxation at *ca.* −80°C, due to a possible overlapping with the PCL glass transition for the original sample (25°C).

Morphological characterisation

Small-angle X-ray scattering. In order to probe the phase structure of the PCL/TEOS ceramers, SAXS experiments have been carried out and some SAXS profiles are shown in *Figures 7–10*. The scattered intensity (I) is plotted against the angular scattering variable, s, which is defined as $s = (2\sin\theta)/\lambda$, where θ is half the radial scattering angle (or the internal scattering angle) and λ is the wavelength of the X-ray beam.

Effect of curing conditions. Figure 7 shows that a scattering maximum is observed in the SAXS profile of a ceramer originally containing 80 wt.% TEOS not only after reaction at 25°C but also after curing at 100°C. Thus a rather periodic fluctuation in the electron density is responsible for a correlation length in the system, in agreement with a

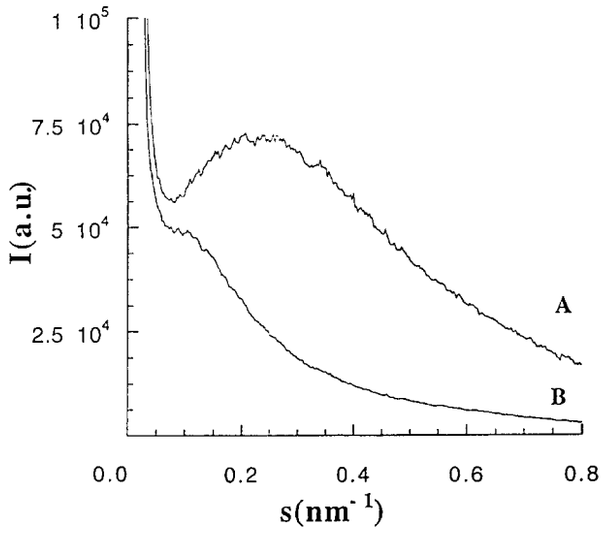

Figure 9 SAXS profiles of ceramers prepared from 80 wt.% TEOS and 20 wt.% PCL (M_n = 2000) end-capped with triethoxysilane (a) and hydroxyl groups (b). Curing at 100°C for 2 days

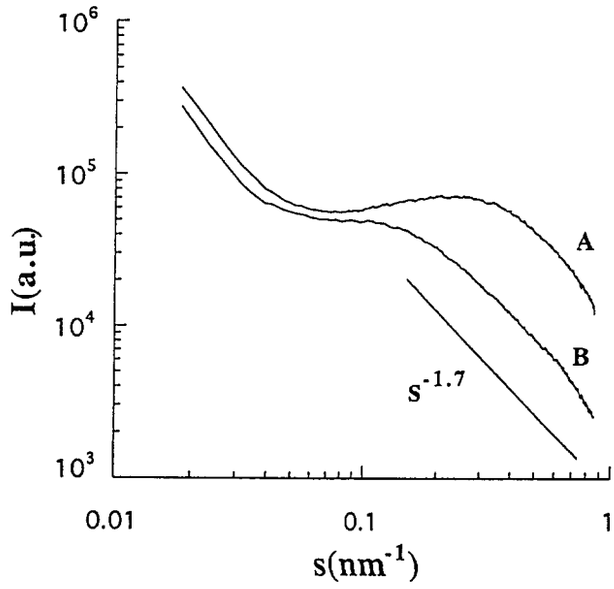

Figure 10 Log–log plots of SAXS intensity *versus* the scattering factor s for the ceramers studied in Fig. 9

microscopic phase separation between PCL and silica. This correlation length is calculated as the reverse of the scattering parameter s at which the maximum is observed.

The correlation distance calculated from *Figure 7* is 3.7 nm for the sample prepared at 25°C and 4.2 nm after curing at 100°C for 2 days. In parallel, the peak intensity is strongly decreased as result of curing. This observation indicates that, in spite of a substantial progress in the reaction, the curing at 100°C of the TEOS/PCL hybrid material does not significantly change the periodicity of the phase morphology, in contrast to the electronic density fluctuation which is much smaller in a possible agreement with an improved homogeneity as result of a much more complete condensation reaction.

Effect of PCL content. *Figure 8* compares the SAXS profiles for TEOS/PCL ceramers of different PCL contents. The scattering intensity rapidly decreases with the PCL content to the point where the scattering maximum goes essentially unresolved when the PCL content is as low as 5 wt.%. The correlation length also decreases from 4.2 nm to 3.0 nm when the PCL content is decreased from 20 to 10 wt.%. Thus a lesser amount PCL seems to be more intimately (homogeneously) distributed within the silica network, which is in a qualitative agreement with DMA measurements.

Effect of PCL functional end-groups. The effect of the PCL reactive end-groups on the SAXS profile is shown in *Figure 9*. When hydroxyl end-groups are substituted for triethoxysilanes all the other conditions being the same, the correlation length increases from 4.2 nm up to 9.5 nm. As previously discussed[1,3], the PCL hydroxyl end-groups are less reactive than the silanolate ones so that the chemical bonding of PCL to silica is less efficient and the intermixing of the two components less intimate. It must be noted that the lower reactivity of the hydroxyl PCL end-groups compared to the triethoxysilone ones is more favourable to self-condensation of TEOS rather than to cross-reaction of TEOS with end-functional PCL, which must unavoidably affect the phase morphology.

A log–log plot of the SAXS intensities *versus* the scattering vector s is shown in *Figure 10*. The analysis of the limiting power law in the Porod region of the scattering curves can provide some information on the interface in the TEOS/PCL hybrid materials. Indeed, in case of fractal structures, the SAXS intensity $I(s)$ agrees with the following power laws[17]

$$\text{mass fractal} \quad I(s) \sim s^{-D_m}, \quad 1 < D_m < 3$$

$$\text{surface fractal} \quad I(s) \sim s^{-(6-D_s)}, \quad 3 < 6 - D_s < 4$$

where D_m is the mass fractal dimension and D_s is the surface fractal dimension.

Figure 10 shows that each scattering profile approaches a limiting slope of 1.7 for curve A and 1.6 for curve B, respectively, indicating that the interface structure is mass fractal whatever the reactivity of the PCL end-groups. This conclusion is consistent with the hydrogen bonding of the ester groups of PCL and OH groups of the silica network. Since the association of PCL and silica phases must be space-filling, PCL has to be intimately mixed with the silica network.

It is worth recalling that Brinker and Scherer[18] have proposed the initial formation of chain-like or lightly branched molecules when TEOS is hydrolysed with small amounts water (e.g. H_2O:Si $\geq$ 5; in this study, H_2O:Si = 4) in the presence of an acid. These molecules then undergo further condensation with formation of a dense network which is classified as fractal[19]. Dilute acidic solutions of 'polymeric' silicon alkoxide can grow by reaction-limited cluster–cluster aggregation (RLCCA)[19–21]. Thus not all collisions result in effective condensation (i.e. permanent bond). The fractal dimension (D) for a RLCCA mechanism is typically between 2.0 and 2.1. Slightly more open structures are formed by diffusion-limited cluster–cluster aggregation (DLCCA)[19,20], whereby clusters become permanently attached upon first contact. In the case of DLCCA, D = 1.8. For the TEOS/PCL system the TEOS polycondensation also occurs in dilute acidic solution, so that a fractal dimension intermediate between the values predicted for the two aggregation models (i.e. RLCCA and DLCCA) would be reasonable. Nevertheless, chemical and/or hydrogen bonding is likely to retard phase separation, and to alter

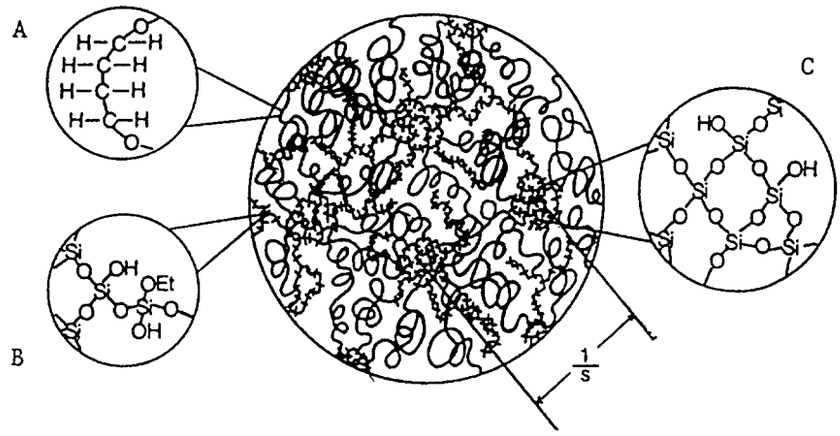

Figure 11 Wilkes' model for TEOS/PTMO hybrid system, (a) PTMO chain, (b) linear species based on partially condensed TEOS, (c) cluster formed by highly condensed TEOS. 1/*S* corresponds to the correlation length observed in SAXS profiles

the aggregation mechanism of the inorganic reagent of the TEOS/PCL system, which can account for a fractal dimension smaller than expected for neat TEOS under acidic conditions.

Wilkes *et al.*[13] have proposed a model for the morphology of TEOS/PTMO hybrid materials which relies upon the formation of microdomains of highly condensed TEOS (*Figure 11*). The correlation length would then be the average interdomain spacing. It must be noted that, in this work, the initial weight percentages of reactants have been used to express the composition of the hybrid materials. However, these values are not the final composition of the dried samples. Since 71.2% of the reactive mass is lost by converting TEOS to SiO_2, the final inorganic glass content (SiO_2) is less than indicated by the initial TEOS weight percentage and easily calculated.

Wilkes' model (*Figure 11*) is based on a final SiO_2 content lower than 40 wt.% and on dominant interaction of the silica network with the polymer chain ends (covalent bonding). In this study, the final SiO_2 content is higher than 50 wt.%, and in addition to the functional end-groups of PCL, the ester groups along the PCL chains can also interact with the silica network. Therefore, the interface structure is mass fractal in TEOS/PCL hybrid materials and the correlation length (*ca.* 4 nm)is smaller than for the TEOS/PTMO system (5–18 nm). Although Wilkes' model can explain why the correlation length of the TEOS/PCL hybrid materials increases with PCL content and when the reactivity of the PCL end-groups is increased, it cannot account for an increasing correlation length with decreasing PCL molecular weight (*Figure 7*b and *Figure 9*b). In reference to Wilkes' model, SiO_2 would form highly branched and possibly interconnected domains in the TEOS/PCL hybrid materials.

A bicontinuous two-phase model suggested by Landry *et al.*[14] is shown in *Figure 12*. The origin of the SAXS maximum would be either the average distance between the constitutive particles or a dominant wavelength for a concentration fluctuation, as observed for a spinodal decomposition. In the two cases, the SAXS peak position is related to the distance between the junction points of the crosslinked organic polymer. This model could also explain why the correlation length of the TEOS/PCL hybrid materials increases with PCL content and when the reactivity of the PCL end-groups is increased, but not the increase of the correlation length when the PCL molecular weight is decreased. Nevertheless, a co-continuous two-phase morphology has been observed for the SiO_2/PCL system by TEM and TEM image analysis (see bellow), at least when the weight composition is close to 50%, which better fits the Landry's model.

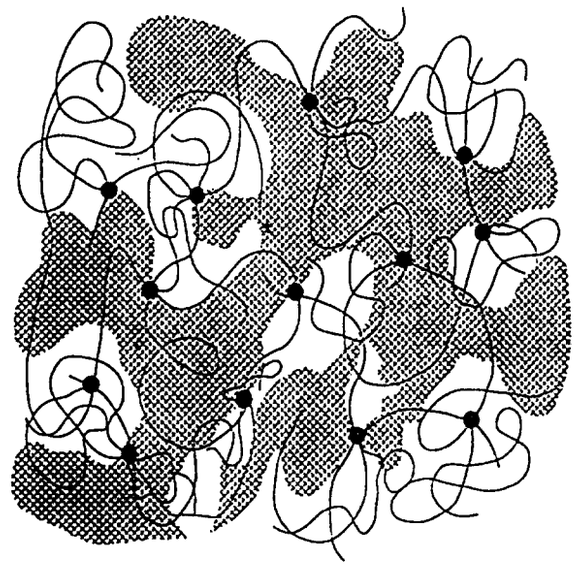

Figure 12 Landry's model for the morphology of an organic–inorganic composite hybrid based on the simulation results for SAXS profiles. It features co-continuous inorganic fractal (shaded region) and organic polymer phases. Microphase separation is proposed to occur by localisation of the inorganic phase in the mesh regions of the cross-linked polymer. Some attachment of the inorganic alkoxides to the functional sites on the polymer (●) is possible

TRANSMISSION ELECTRON MICROSCOPY AND IMAGE ANALYSIS

The transmission electron micrograph of a TEOS/PCL ceramer is shown in *Figure 13* at a magnification of 105 000. This observation suggests at least some co-continuity in the phase structure for this material of a weight composition close to 50% SiO_2. TEM images of hybrid materials with a higher silica content, i.e. higher than 70 wt.%, do not show characteristic structural features any more due to the poor contrast between the organic polymer and inorganic phases. More information about the phase morphology of the TEOS/PCL ceramers analysed in *Figure 13* has been searched for by image analysis. *Figure 14* shows magnification of two regions of the TEM micrograph

and the related binary images, in which PCL is seen as white pixels and silica as black pixels.

The statistical image analysis has been performed using the covariance function $C(X,\lambda)$[15] for the binary image, which underscores the non-homogeneity of the spatial distribution of the two complementary phases. The covariance $C(X,\lambda)$ of a stationary random function $f(x)$ is defined as the probability that two points x and $x + <8,23>$ belong to the same phase A. $C(X,\lambda)$ has the following properties: $C(X,0) = p$ where $p = \text{Prob.}\{x \in A\}$, $C(X, 0) \geq C(X,\lambda)$, $C(X,\lambda) \rightarrow p^2$ when $\lambda \rightarrow \infty$. The way $C(X,\lambda)$ passes from p to p^2 in relation to the modulus and direction of λ provides structural information. By definition, $C(X,0)$ is the concentration of the studied phase and, for convex objects, the derivative of the covariance function taken at the origin $C'(X,0)$ is related to the specific (per surface unit) perimeter of the studied phase $U(X)$ by[15]

$$U(X) = -\frac{1}{2}\int_0^{2\pi} C'(X,0)\,\mathrm{d}\alpha \qquad (1)$$

where α is the angle of the vector λ.

When two materials of the same phase composition are compared, a larger slope of $C(X,\lambda)$ near the origin indicates a finer structure. Oscillations in this $C(X,\lambda)$ function is indicative of a structure with a characteristic length (sizes, periodicities, etc.) and the directional character of $C(X,\lambda)$ allows anisotropy in the phase distribution to be detected. The covariance function $C(\lambda)$ for the binary images has been calculated using the following algorithm[16]

$$C(l) = \frac{A(Mb \cap Mb')}{A(Z \cap Z')} \qquad (2)$$

where Mb is the binary image studied, Z is the digital mask in which the covariance of the digital set Mb is measured; Mb', and Z' are the corresponding values after translation over a distance λ.

Figure 15 shows the silica (silica, white pixels; PCL, black pixels) and PCL (silica, black pixels; PCL, white pixels) covariance curves as calculated with the algorithm in

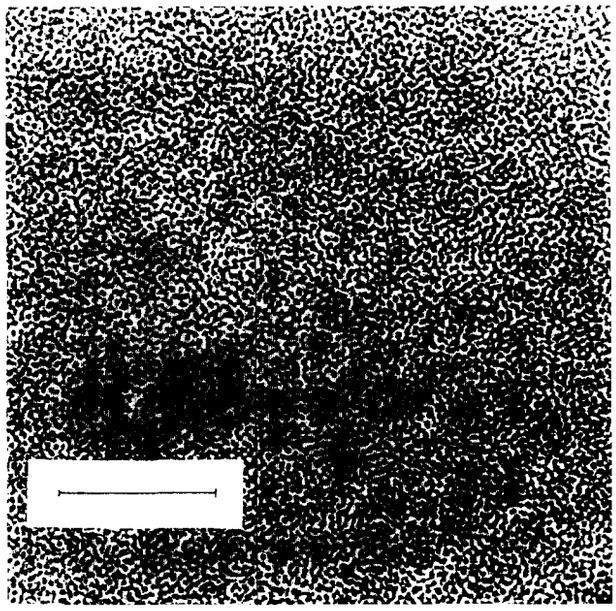

Figure 13 Transmission electron micrograph (magnification of 105 000) for a PCL ceramer containing 54 wt.% SiO_2. The length of the bar is 100 nm. SiO_2 is the dark component part

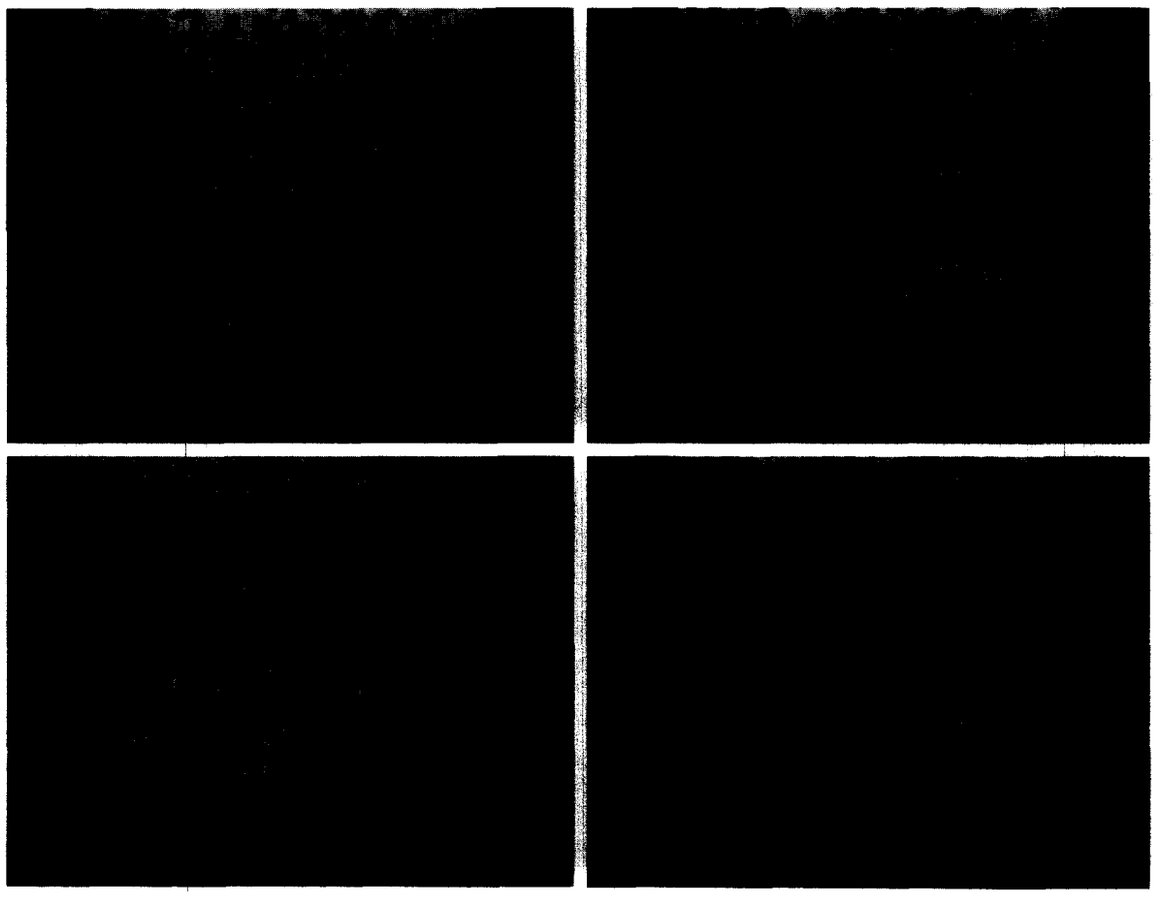

Figure 14 Magnification of two regions of the TEM micrograph (left side) shown in Fig. 13 and their binary images (right side)

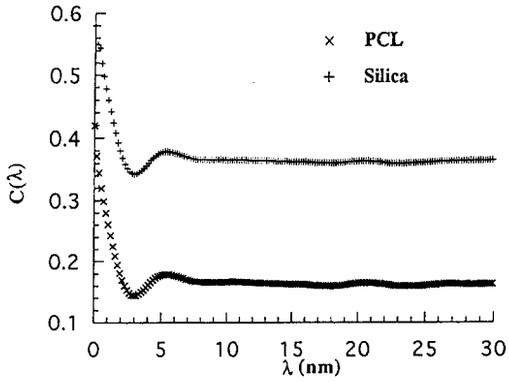

Figure 15 Covariance curves for silica (silica, white pixels; PCL, black pixels) and PCL (silica, black pixels; PCL, white pixels)

equation (2). Concentration $C(X,0)$ of the phases on the images is 0.42 and 0.58 for the PCL and silica, respectively, in good agreement with the actual concentration, pointing out the homogeneity of the sample.

Both curves can be superimposed so that the complementary silica and PCL networks have the same morphology. The oscillations observed confirm the existence of a characteristic length for the two-phase structure. The distance between the two first maxima (λ) is the average distance between the elements of the analysed structure. $\lambda = 5$ nm is found from the silica covariance function, and the PCL covariance curve agrees with $\lambda = 5.5$ nm. These measurements indicate that the silica and PCL networks are intimately interwoven in a co-continuous organisation of the phases.

CONCLUSION

From the dynamic mechanical analysis, an increasing reactivity of the PCL end-groups, i.e. triethoxysilane instead of hydroxyl end-groups, results in a higher glass transition temperature for the organic component and a slight increase in modulus in the whole temperature range. Both the modulus of ceramer and the glass transition temperature of PCL slightly increase with the number of functional end-groups per PCL chain. The dynamic mechanical properties of the final ceramers are not very sensitive to PCL molecular weight which confirms that intermolecular PCL/silica cross-interactions play the decisive role on the PCL chain mobility (T_g) and phase separation. A decrease in the PCL content from 20:80 to 10:90 (wt/wt, PCL/TEOS) results in an increase in both the modulus and the glass transition temperature of PCL. At low PCL content, i.e. 5:95 (wt/wt, PCL/TEOS), the observation of the PCL glass transition by dynamic mechanical analysis becomes a problem. Curing at 100°C of the ceramers prepared at 25°C shows a shift of the PCL glass transition toward higher temperature and an increase of the modulus beyond that transition.

The SAXS results indicate that a correlation length is observed for the hybrid materials, which decreases with the PCL content and when the reactivity of the PCL end-groups is increased. When the PCL content is low enough, i.e. 5:95 (wt/wt, PCL/TEOS), the SAXS profiles become so 'smooth' that no maximum can be detected any more. The limiting Porod slope is about 1.7 indicating that the PCL/SiO2 interface is mass fractal, in agreement with a co-continuous structure.

TEM observations and TEM image analysis agree with a co-continuous interpenetrating network of the inorganic component (silica) and the organic polymer (PCL), at least when the weight composition is close to 50% (SiO_2/PCL). An average distance of 5 nm between the constitutive components in case of a 50/50 weight composition has been calculated. The surface morphology of TEOS/PCL hybrid materials analysed by atomic force microscopy before and after selective etching of PCL and silica will be reported in the future.

ACKNOWLEDGEMENTS

The authors are very much indebted to the 'Services Federaux des Affaires Scientifiques, Techniques et Culturelles' for general support to CERM and a fellowship to TD in the frame of the 'Poles d'Attraction Interuniversitaires Polymeres'. They warmly thank R. Sobry, B. Diez and P. Van den Bossche for SAXS measurements (Laboratory of Experimental Physics, Liege, Belgium).

REFERENCES

1. Tian, D., Dubois, Ph. and Jérôme, R., *Polymer*, 1996, **37**, 3983.
2. Tian, D., Dubois, Ph., Grandfils, Ch., Jérôme, R., Viville, P., Lazzaroni, R., Brédas, J. L. and Leprince, P., *Chem. Mater.*, 1997, **9**, 871.
3. Tian, D., Dubois, Ph. and Jérôme, R., *J. Polym. Sci., Polym. Chem.*, 1997, **35**, 2295.
4. Schindler, A., Jeffcoat, R., Kimmel, G. L., Pitt, C. G., Wall, M. E. and Zweidinger, R., *Biodegradable Polymer for Sustained Drug Delivery*. In: eds Pearce, J. R., Schaefger, E. M., *Contemporary Topics in Polymer Science*, Vol. 2. Plenum, New York, 1977, p. 251.
5. Vert, M., *Makromol. Chem., Macromol. Symp.*, 1986, **6**, 109.
6. Pak, J., Ford, J. L., Rostron, C. and Walters, V., *Pharm. Acta Helv.*, 1985, **60**(5), 160.
7. Grijpma, D. W., Zondervan, G. J. and Pennings, A. J., *Polym. Bull.*, 1991, **25**, 327.
8. Dubois, Ph., Degée, Ph., Jérôme, R. and Teyssié, Ph., *Macromolecules*, 1993, **26**, 2730.
9. Tian, D., Dubois, Ph., Jérôme, R. and Teyssié, Ph., *Macromolecules*, 1994, **27**, 4134.
10. Tian, D., Dubois, Ph., Grandfils, Ch. and Jérôme, R., *Macromolecules*, 1997, **30**, 406.
11. Tian, D., Dubois, Ph. and Jerome, R., *Macromolecules*, 1997, **30**, 2575.
12. Huang, H. H., Wilkes, G. L. and Carlson, J. G., *Polymer*, 1989, **30**, 2001.
13. (a) Huang, H. H., Raymond, H. G., and Wilkes, G. L., *ACS Symposium Series* 1987, **360**, 354; (b) Huang, H. H., Wilkes, G. L., *Polym. Bull.* 1987, **18**, 455.
14. Landry, M. R., Coltrain, B. K., Landry, C. J. and O'Reilly, J. M., *J. Polym. Sci. Part B, Polym. Phys.*, 1995, **33**, 637.
15. Serra, J. *Image Analysis and Mathematical Morphology*, Vol. 1. Academic Press, New York, 1982.
16. Coster, M. and Chermant, L. *Precis d'analyse d'images*. CNRS, Paris, 1985.
17. Martin, J. E. and Hurd, A. J., *J. Appl. Cryst.*, 1987, **20**, 61.
18. Brinker, C.J. and Scherer, G.W., *J. Non-Cryst. Solid*, 1985, **70**, 301.
19. Brinker, C. J. and Scherer, G. W., *Sol–gel science*. Academic Press, San Diego, CA, 1990.
20. Meakin, P., *Ann. Rev. Phys. Chem.*, 1988, **39**, 237.
21. Schaefer, D. W., Martin, J. E. and Keefer, K. D., in eds Bocarra, N. and Keefer, K. D., *Physics of Finely Divided Matter*. Springer-Verlag, Berlin, 1986, p. 31.